Analyzing the Stability of Aluminium Electrolysis Cells Using a Mechanical Model

Ibrahim Mohammad[1], Marc Dupuis[2] and Valdis Bojarevics[3]
1. Assistant Professor of Instruction
Department of Mechanical Engineering – University of Rochester, Rochester, USA
2. Consultant
GeniSim, Jonquière, Canada
3. Professor
University of Greenwich, London, United Kingdom
Corresponding author: ibrahim@imconsultingservices.net
https://doi.org/10.71659/icsoba2024-al057

Abstract

The magnetohydrodynamic (MHD) stability of an aluminium (Al) electrolysis cell is important for overall stable operation at a lower anode-to-cathode distance (ACD). In particular, it is beneficial to understand the influence of changing cell parameters such as the ACD and cell amperage on the stability of the cell, which can be quantified by the growth or decay rate of the interfacial waves on the Al-electrolyte interface. This can be done by running a suite of numerical MHD simulations with different cell parameters and then using the resulting interface evolution to find the growth/decay rates. However, with many combinations of cell parameters to test, such an endeavor will often be expensive and time consuming. In this work, we utilize the mechanical model of MHD instabilities in Al cells presented in [1] to analyze the stability of a TRIMET 180 kA Al cell for different combinations of ACD and cell amperage. We first show that the model's stability and growth/decay rates can be found quickly by solving an algebraic equation for the complex frequencies of oscillation. Then, we calibrate the model to the parameters of the TRIMET 180 kA cell and study its stability at different ACD and cell amperage combinations. We show a 2D stability map of the growth/decay rates and a 3D stability surface. For a few ACD and anodic current density (cell amperage) combinations, we simulate the TRIMET 180 kA Al cell using MHD-Valdis to find the Al-electrolyte interface growth/decay rate. We show that the growth/decay rates from the mobile model match those from MHD-Valdis simulations. Our results show the value of using the mechanical model as a complement tool to MHD simulations, where it can be used to rapidly narrow down the combinations of cell parameters to be simulated numerically.

Keywords: Magnetohydrodynamic instability, Aluminium cell modelling, Metal pad instability

1. Introduction

The overall stability of aluminium (Al) electrolysis cells relies on the stability of three coupled dynamical phenomena: magnetohydrodynamic (MHD), chemical, and thermal [2]. This stability must be maintained as cell parameters are changed for better energy and current efficiency. In particular, the cell's energy efficiency can be improved by reducing the electrolyte's thickness, quantified by the anode to cathode distance (ACD) [1]. However, reducing the ACD negatively impacts the MHD stability of the cell, and it could go unstable [3-4], where disturbances on the Al-cryolite interface are amplified reducing the cell's current efficiency and possibly shorting it [2-4]. This MHD instability, known as the metal pad instability (MPI) [4], is a result of horizontal electromagnetic forces in the molten Al coupling orthogonal interfacial wave modes (orthogonal standing waves) having close frequencies [1, 5].

The MPI is influenced by many cell and design parameters such as the ACD, cell amperage, molten Al metal level, vertical magnetic field, and cell aspect ratio [3-4]. Thus, to maintain cell stability, it is important to know how the MHD stability is affected by changing these parameters. To do so, we can numerically simulate the cell using specialized software such as MHD-Valdis [5-7] to check whether a cell is stable/unstable for a given set of cell parameters. We can quantify how stable/unstable the cell is by looking at the evolution rate of the waves on the Al-cryolite interface [4], which if positive indicates growth (instability) and if negative indicates decay (stability). This would allow us to compare the relative stability between any two groups of cell parameters. However, as the number of cell parameter combinations increases, the time and computational costs of simulations become large. This makes it difficult to scan a large parameter space with tens of cell parameter combinations.

A mobile model was presented in [1] as a mechanical analogue of the MPI, and it exhibited stability and instability at realistic cell parameters of a TRIMET 180 kA Al cell. Beyond a binary stable/unstable result for a given set of cell parameters, we wanted to see if the mobile model can accurately capture how stable/unstable the cell is. More specifically, if the growth/decay rate of the mobile model would be similar to that of the Al cell's interface. In this work, we use the mobile model to explore the growth/decay rate of a TRIMET 180 kA cell at different combinations of ACD and anodic current densities (cell amperage). We first show that the stability of the mobile model can be studied directly, in a way that the growth/decay rates can be extracted directly without solving for the mobile's motion. Then, we calibrate the mobile model to a critically stable TRIMET 180 kA cell having the cell parameters in Table 1. We use the calibrated mobile to find the growth/decay rates at over 100 combinations of ACD and anodic current densities, creating a 2D stability map. Finally, we simulate the TRIMET 180 kA cell for a few combinations (see Table 2) in MHD-Valdis [5-7] and compare the interface growth/decay rates to those from the mobile model.

Table 1. TRIMET 180 kA cell parameters, reproduced from [1].

J_0 (A/cm^2)	B_z (T)	h_0 (m)	L_x (m)	L_y(m)	H (m)
0.8	0.003	0.043	7.92	3.57	0.17

where:

J_0 Nominal current density in bath, A/m^2
B_z Vertical constant and uniform magnetic flux density, T
h_0 Thickness of the cryolite or ACD, m
L_x Length of the Al plate in the x direction, m
L_y Length of the Al plate in the y direction, m
H Thickness of the Al plate (analogous to metal pad height), m.

2. Mobile Model

2.1 Brief Description

The mechanical model of the MPI given in [1] is a mobile, shown in Figure 1. It consists of a broad and thin rectangular Al plate (representing the Al layer) that has a variable center of mass (COM) and it is subjected to a damping torque. The Al plate is connected to a fixed ceiling (representing the anodes) by a massless, rigid strut, and can swing about the x and y axes (horizontal axes) with the pivot as shown in Figure 1. The gap between the Al plate and the fixed ceiling is filled with massless and frictionless cryolite (representing the electrolyte layer) creating a path for a steady and uniform current density of magnitude J_0 to pass vertically downwards from the fixed ceiling to the Al plate. The entire mobile is subjected to an external constant and uniform vertical magnetic flux density of magnitude B_z.

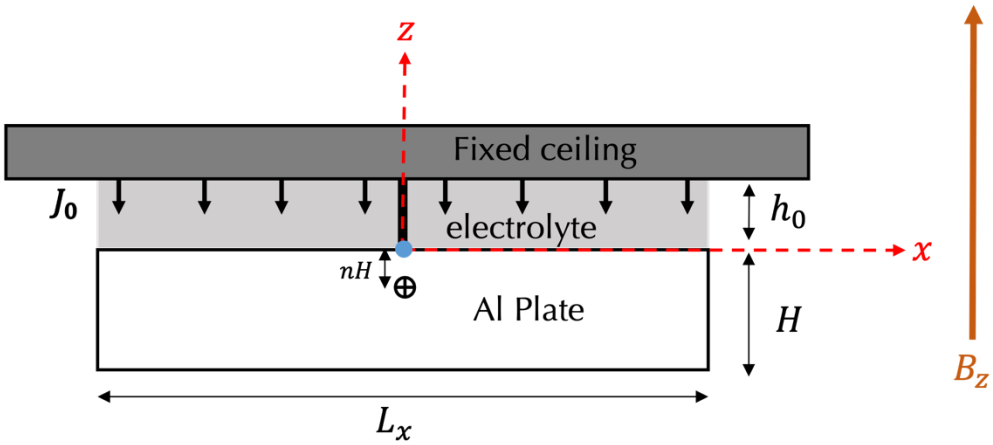

Figure 1. Mobile model of the MPI [1] at equilibrium state. The pivot point is indicated by a blue disc and the Al plate's COM by a circle with a cross.

where:

n Relative position of the COM measured from the top, unitless.

Naturally, when there is no current (or the vertical magnetic flux density is absent) if the Al plate is tilted from its equilibrium position, the gravitational force will push the Al plate back towards the equilibrium position. The Al plate will oscillate at its natural gravitational frequency in each horizontal direction until it rests back at its equilibrium due to the damping torque applied on the mobile [1]. However, when the current is present, tilting the Al plate creates a horizontal perturbation in the Al plate's current density (see Figure 2). This horizontal current density interacts with the vertical magnetic flux density to generate a horizontal electromagnetic force acting on the Al plate that couples the Al plate's motion in the x and y directions [1]. If strong enough, this coupling can lead to the Al plate oscillating at the same frequency in both directions which consequently leads to unstable motion. This physical picture is quite similar to what happens in an Al electrolysis cell, where horizontal electromagnetic forces generated in the molten Al may couple gravitational wave modes having close frequencies, leading to unstable motion of the molten Al [3–5, 8].

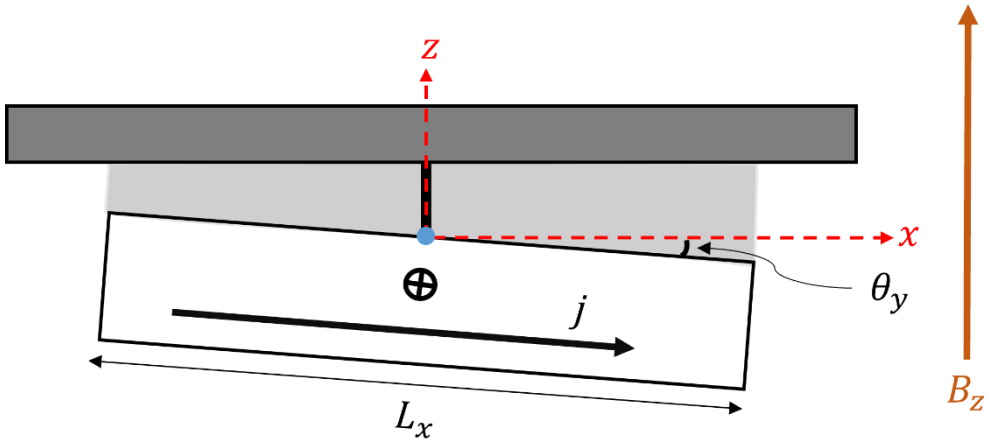

Figure 2. Mobile model at a small θ_y rotation about y axis. A perturbated current density (j) is generated inside the Al plate as shown.

If we consider small rotations θ_x and θ_y (shown in Figure 2) about the x and y axes, respectively, then the mobile's motion can be described by a coupled system of second order ordinary differential equations (ODEs) [1]

$$\ddot{\gamma}_x + 2\zeta\omega_x\dot{\gamma}_x + \omega_x^2\gamma_x = -a\gamma_y \quad (1)$$

$$\ddot{\gamma}_y + 2\zeta\omega_y\dot{\gamma}_y + \omega_y^2\gamma_y = \quad a\gamma_x \quad (2)$$

where:

ζ Damping coefficient, unitless
ω_x Natural gravitational frequency in the x direction, rad/s
ω_y Natural gravitational frequency in the y direction, rad/s
a Electromagnetic coupling parameter, 1/s^2

and

$$\gamma_x = \frac{\theta_x}{L_x^2} \quad (3)$$

$$\gamma_y = \frac{\theta_y}{L_y^2} \quad (4)$$

The natural gravitational frequencies (ω_x, ω_y) and the electromagnetic coupling parameter (a) are parameters inferred directly from the cell parameters (h_0, H, L_x, L_y, J_0, B_z), where [1]

$$\omega_x^2 = \frac{12ngH}{L_y^2} \quad (5)$$

$$\omega_y^2 = \frac{12ngH}{L_x^2} \quad (6)$$

$$a = \frac{(h_0+nH)J_0B_z}{\rho_{al}Hh_0} \quad (7)$$

where:

L_y Length of the Al plate in the y direction, m

While the relative COM position, n, and the damping coefficient, ζ, are calibration parameters that can be adjusted so that the mobile is critically stable at the correct cell parameters.

2.2 Mobile Calibration

The mobile model was calibrated to the TRIMET 180 kA cell such that critical stability is achieved for the cell parameters in Table 1, where critical stability is when the waves of the Al-cryolite interface neither grow nor decay in time [4]. In [1] this was done by varying ζ to achieve 90 % damping of the pure gravitational oscillation (*i.e.*, when no current is present) within 1 period, and adjusting the n such that critical stability is at the correct parameters. Here, since we are interested in growth/decay rates of the mobile's motion, we used a different procedure that we believe better captures the physics of the MPI.

Disturbances on the Al-electrolyte interface can be represented as a sum of different interfacial waves modes, each is a standing wave with an integer pair (m, n) of wave mode numbers and a frequency [4–5]. There is an infinite number of such modes, and the MPI involves a resonance of modes where the electromagnetic forces couple two or more interfacial wave modes having similar frequencies [3–4,8]. For example, the MHD-Valdis simulation results from [4] of the same TRIMET 180 kA cell showed that the MPI is a coupling between the (2,0), (0,1) and (1,1) modes. Due to the rigid nature of the mobile, only one mode is possible in each direction, namely the equivalent of the (1,0) and (0,1) modes in an Al cell. The (1,0) mode has frequency ω_x and the

(0,1) mode has frequency ω_y, which given the cell dimensions in Table 1 are not close. Since the MPI resonance involves modes of similar frequencies, we want the two modes on the mobile to have similar frequencies.

Hence, when calibrating the mobile, we first adjusted the COM such that the mobile is critically stable at the TRIMET 180 kA Al cell parameters in Table 1 with no damping ($\zeta = 0$). As in [1], we found the mobile to be critically stable at $n = 0.1621$ when no damping is present. Then, we divided the cell's length (L_x) by 2 so that ω_x and ω_y are close to one another. One can think about dividing by 2 as wanting the (2,0) oscillation mode in the Al cell to be the (1,0) mode in the mobile model. Making the aspect ratio closer to one makes the critically stable mobile to become unstable. Finally, we adjust the damping coefficient, ζ, so that critical stability is regained at the cell parameters of Table 1. This occurred at $\zeta \sim 0.213$.

2.3 Quantifying Motion Stability

To check whether the mobile model is stable or not for a given set of cell parameters, we can solve the system of Equation (1) and Equation (2) numerically using MATLAB to find the mobile's motion, and then fit an exponential function to the result, as shown in Figure 3. Since we are only interested in the stability of the mobile and the growth/decay rates of its motion, it would be more efficient to get the rates without solving for the mobile's motion.

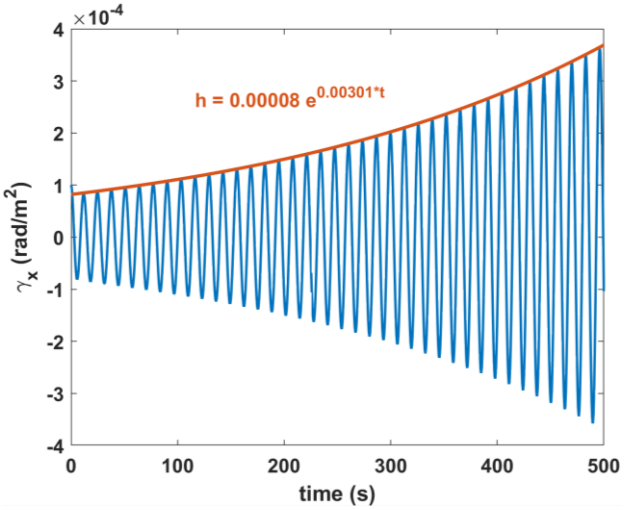

Figure 3. Example of mobile motion with an exponential fit on the peaks to the find the growth rate. This mobile is at 4 cm ACD and 0.8 A/cm² for J_0.

Luckily, we can find the growth/decay rates directly from Equations (1-2) by assuming a solution with a complex exponential in time:

$$\gamma_x = \tilde{\gamma}_x e^{i\omega t} \tag{8}$$

$$\gamma_y = \tilde{\gamma}_y e^{i\omega t} \tag{9}$$

where:

$\tilde{\gamma}_x$ Amplitude of γ_x , rad/m²
$\tilde{\gamma}_y$ Amplitude of γ_y , rad/m²
ω Complex frequency of oscillation, rad/s

The complex frequency can be written in terms of its real and imaginary parts as:

$$\omega = \omega_{\text{real}} + i\omega_{imaginary} \tag{10}$$

The real part, ω_{real}, determines the frequency of the mobile's motion, while the sign of the imaginary part, $\omega_{imaginary}$, determines the stability of the mobile motion. Specifically, if it is positive, then the motion is stable, and if it is negative, the motion is unstable.

Substituting Equations (8, 9) into Equations (1, 2) and reducing, we can write the resultant system as a matrix equation:

$$\begin{bmatrix} -\omega^2 + 2\zeta\omega_x i\omega + \omega_x^2 & a \\ -a & -\omega^2 + 2\zeta\omega_y i\omega + \omega_y^2 \end{bmatrix} \begin{bmatrix} \gamma_x \\ \gamma_y \end{bmatrix} = \begin{bmatrix} 0 \\ 0 \end{bmatrix} \tag{11}$$

For a non-trivial solution ($\gamma_x, \gamma_y \neq 0$), the determinant of the coefficient matrix must be 0. Hence, we find the fourth order equation for ω

$$\omega^4 - \left(2\zeta\omega_x + 2\zeta\omega_y\right)i\omega^3 - \left(\omega_x^2 + \omega_y^2 + 4\zeta^2\omega_x\omega_y\right)\omega^2 + \left(2\zeta\omega_x\omega_y^2 + 2\zeta\omega_x^2\omega_y\right)i\omega + \omega_x^2\omega_y^2 + a^2 = 0 \tag{12}$$

We can solve Equation (12) numerically and directly extract the growth/decay rate of the mobile's motion. This is simpler and much quicker than having to solve a coupled system of second order ordinary differential equations (ODEs), Equations (1, 2), for the mobile's motion and then fitting an exponential function to the result.

3. Results

3.1 Stability Map: ACD vs Anodic Current Density (Cell Amperage)

We wanted to use the calibrated mobile model of the TRIMET 180 kA cell to check the stability at different values for the ACD and anodic current density (J_0). We varied the ACD from 3.5 cm to 5 cm in steps of 0.1 cm, and J_0 from 0.72 A/cm^2 to 0.84 A/cm^2 in steps of 0.02 A/cm^2, totaling 112 different combinations. For each combination of (ACD, J_0) and holding all other parameters fixed, we solved Equation (12) numerically using MATLAB for ω and extracted the growth/decay rates of the mobile's motion. The results are summarized in the stability map of Figure 4.

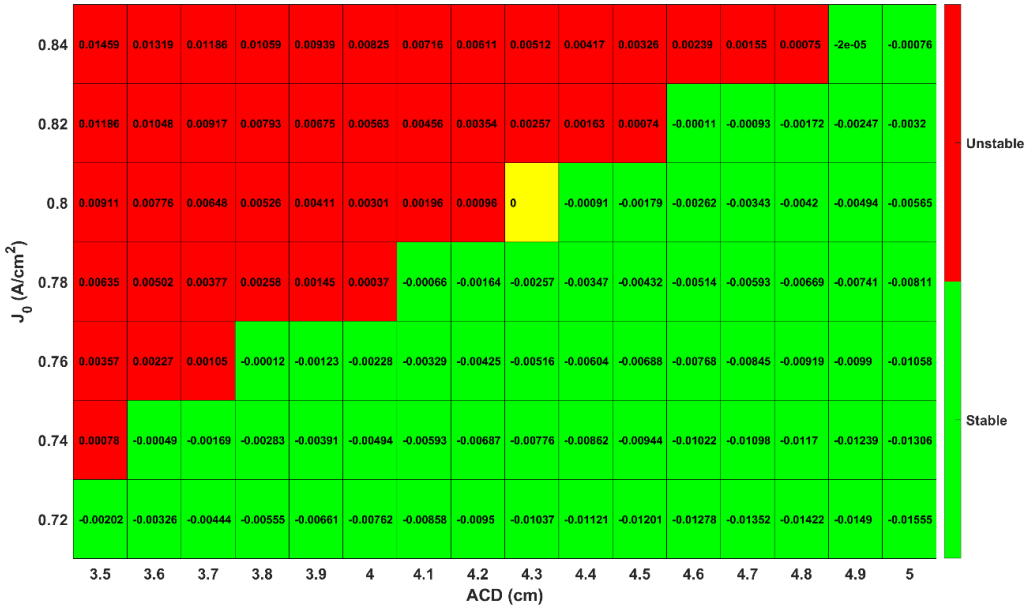

Figure 4. Growth/Decay rates of the mobile model at different ACD and J_0. Critical stability is at 4.3 cm ACD and 0.8 A/cm^2 for J_0.

As expected from the calibration process, the mobile is critically stable at $J_0 = 0.80$ A/cm^2, and ACD of 4.3 cm. Also, Figure 4 shows that increasing the ACD has a stabilizing effect, while increasing the anodic current density has a destabilizing effect. Both observations agree with the situation in a real cell. The same stability map can also be visualized as a 3D stability surface which allows us to visually see the slopes and curvature as ACD and J_0 change.

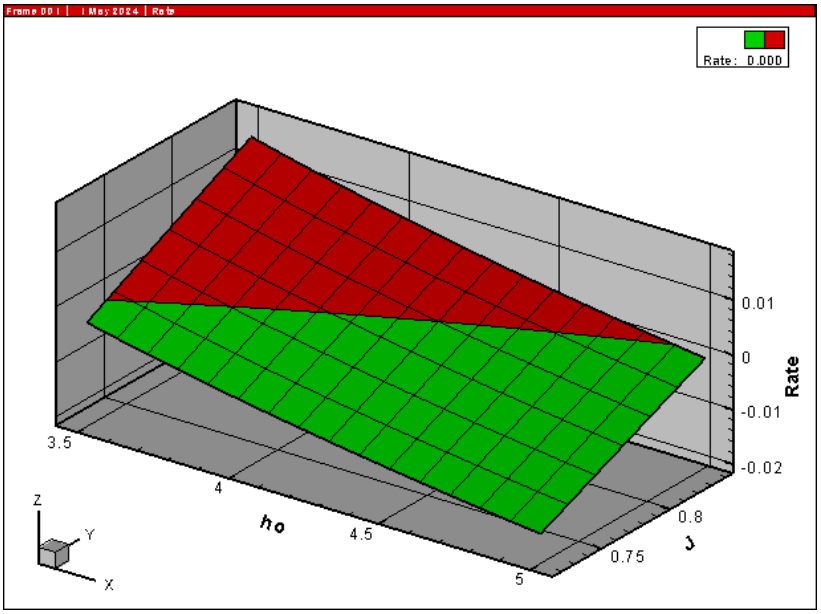

Figure 5. Growth/Decay rates of the mobile model presented as a surface map for the studied range of ACD and J_0.

3.2 MHD-Valdis Simulations

We wanted to see how the growth/decay rates compare to those from simulating the TRIMET 180 kA cell with the same parameters in MHD-Valdis [5-7]. Briefly, MHD-Valdis uses an extended turbulent shallow layer fluids model coupled with 3D electromagnetic fields [5]. We

conducted seven simulations, one of which is at the parameters of critical stability (4.3 cm and 0.8 A/cm^2). For each simulation, we followed the same procedure as in [4] to find the growth/decay rates on the Al-electrolyte interface. Briefly, this procedure involves finding the deviation of the interface shape from its time averaged value (see Figure 6) and then taking a root-mean-square (RMS) of the result, for every time step.

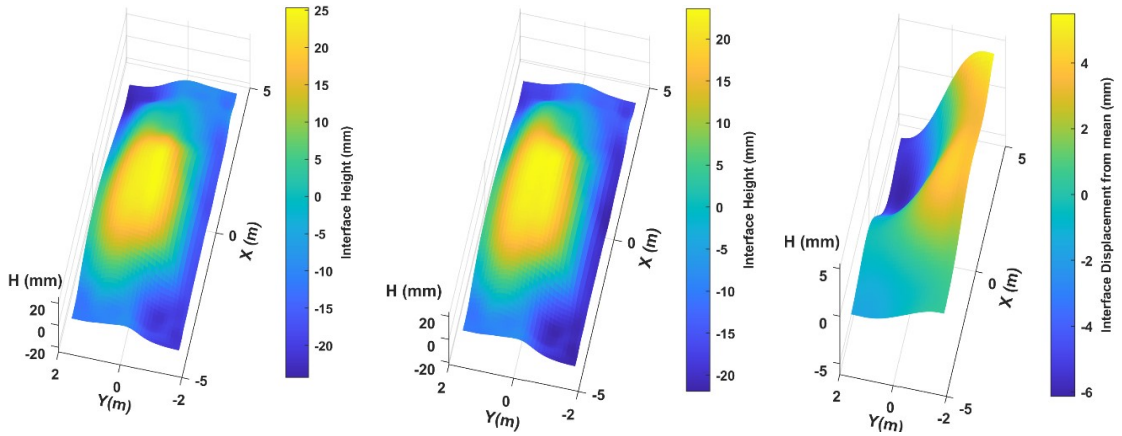

Figure 6. Interface at $J_0 = 0.8$ A/cm^2 and 4.3 cm ACD. Left: Interface shape at 280 s. Middle: Time averaged interface shape. Right: deviation of the interface shape at 280 s from the time averaged shape.

Then, we fit a one term exponential function on the rms interface displacement using MATLAB's built-in function "fit.m", which uses a non-linear least square method [9]. The function returns the coefficients of the exponential fit along with the 95 % confidence interval of each coefficient [9]. We use the exponent from the one term exponential fitting process as the growth/decay rate. The results are shown in Figures 7–10 and summarized in Table 2.

Table 2. Parameters of the TRIMET 180 kA used in MHD-Valdis simulations and the resulting interface evolution rates and 95% confidence interval.

J_0 (A/cm^2)	ACD (cm)	Rate (1/s)	Rate lower bound (1/s)	Rate upper bound (1/s)
0.8	4.3	0.00007	-0.00002	0.00016
0.8	4.5	-0.00199	-0.00212	-0.00185
0.8	4.0	0.00352	0.00301	0.00395
0.72	4.3	-0.01154	-0.01262	-0.01047
0.72	4.0	-0.00853	-0.00934	-0.00773
0.84	4.5	0.00312	0.0028	0.00345
0.84	4.3	0.00477	0.00405	0.00549

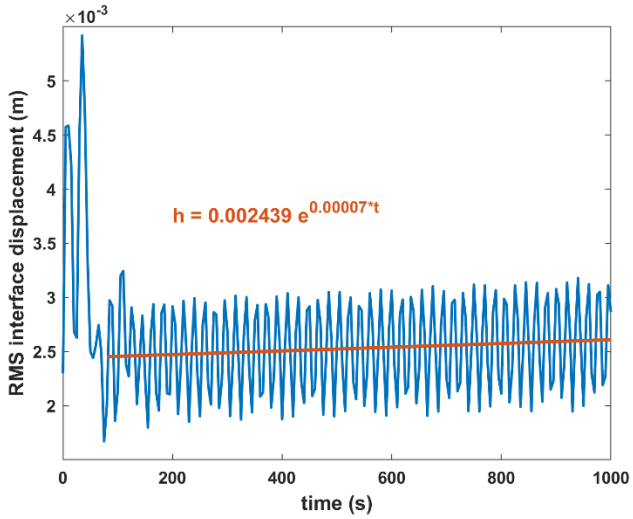

Figure 7. RMS interface displacement at $J_0 = 0.8$ A/cm^2 and 4.3 cm ACD. The cell is critically stable with the exponent ~ 0.

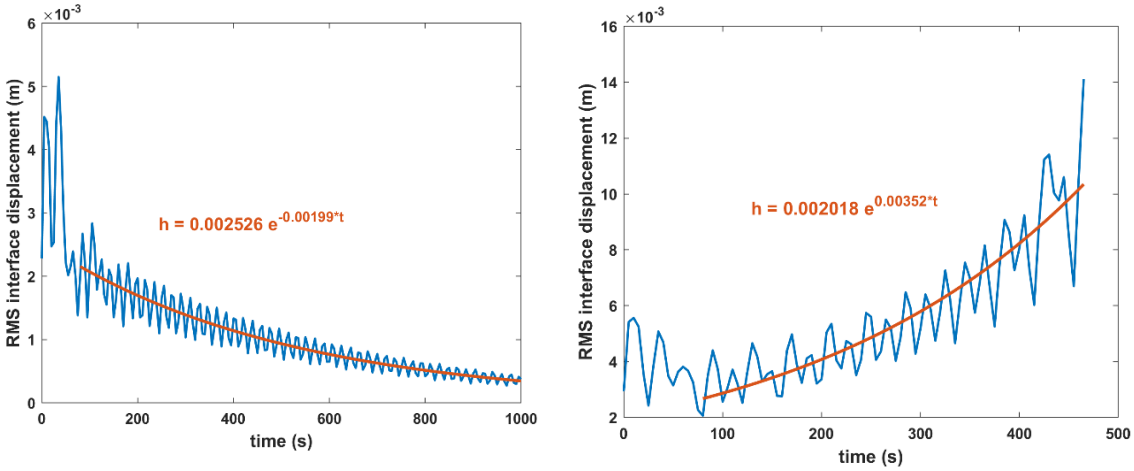

Figure 8. RMS interface displacement at $J_0 = 0.8$ A/cm^2. Left: at 4.5 cm ACD, the cell is stable with the displacement decaying in time. Right: at 4 cm ACD, the cell is unstable with the displacement growing in time.

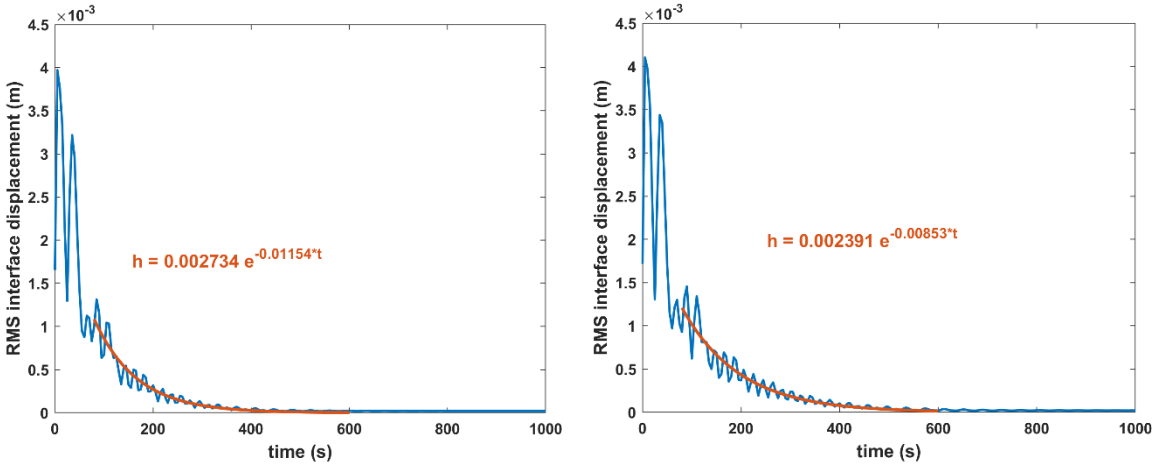

Figure 9. RMS interface displacement at $J_0 = 0.72$ A/cm^2. Left: at 4.3 cm ACD, the cell is stable with the displacement decaying in time. Right: at 4 cm ACD, the cell is stable with the displacement decaying in time, but at a smaller rate.

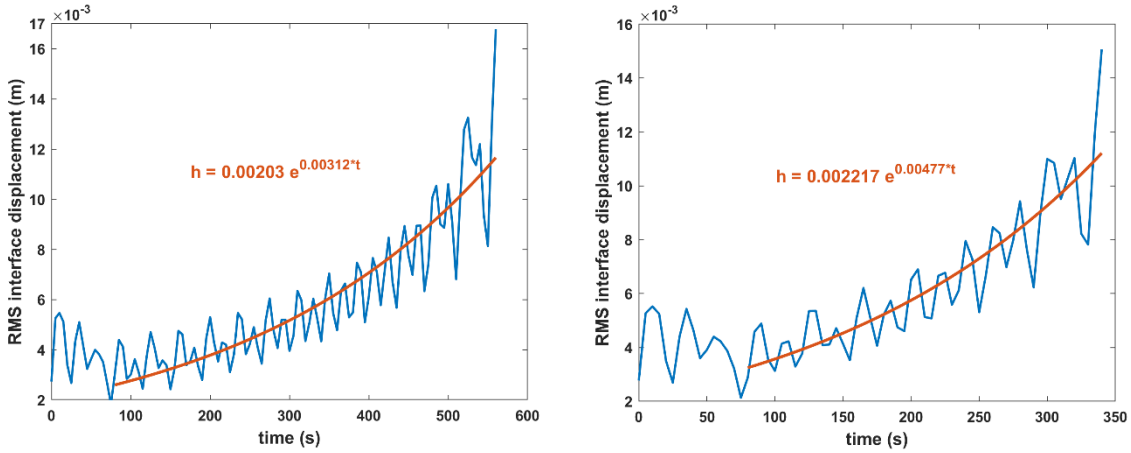

Figure 10. RMS interface displacement at $J_0 = 0.84$ A/cm^2. Left: at 4.5 cm ACD, the cell is unstable with the displacement growing in time. Right: at 4.3 cm ACD, the cell is more unstable with the displacement growing in time at a higher rate than the 4.5 cm ACD case (left).

3.3 Comparing Mobile Model and MHD-Valdis Simulation Rates

For each of the simulations we ran, we plotted the interface growth/decay rates found from the exponential fits along with the 95% confidence interval. Then, we plotted the growth/decay rates from the mobile model at the same ACD and J_0. As shown in Figure 11, the growth/decay rates of the mobile model are very close to those from the MHD-Valdis simulations, almost always falling within the 95% confidence interval.

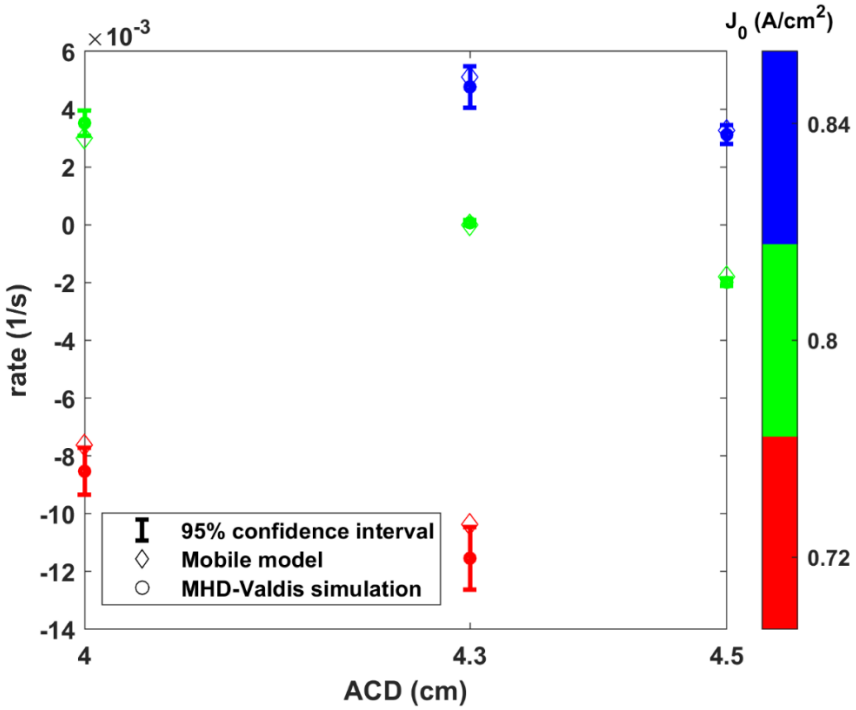

Figure 11. Growth/Decay rates of the interface from MHD-Valdis simulations at different ACD and J_0 combinations with 95% confidence interval overlapped with the growth/decay rates from the mobile model.

4. Conclusions and Future Work

We used the mobile model of the MPI in [1] to investigate the stability of the TRIMET 180 kA Al cells at over a hundred different combinations of ACD and anodic current density combinations (cell amperage). We first used stability analysis to derive an algebraic equation that can be solved to find mobile's growth/decay rate directly, without having to solve for the mobile's motion explicitly. Then, we calibrated the mobile to the parameters of a critically stable TRIMET 180 kA and used it to find the growth/decay rates at different ACD and J_0 values.

The ACD-J_0 stability map showed that increasing the ACD improves stability while increasing J_0 worsens it, as expected. Finally, for six different ACD and J_0 combinations, we compared the mobile model rates to those from simulating a TRIMET 180 kA Al cell with the same parameters in MHD-Valdis. Our results showed that the mobile rates are in good agreement with those from the MHD-VALDIS simulation. This is promising as it has the benefit of rapidly narrowing down the combinations of cell parameters to be simulated numerically, reducing the computational expense.

Our results only compare the growth/decay rates when two parameters are changed: ACD and J_0. It is important to compare rates when other parameters are changed, such as the metal height or magnetic flux density magnitude. Also, the mobile model matched the growth/decay rates of the TRIMET 180 kA cell remarkably well. It would be interesting to see if the mobile model can achieve such good results with other cells, which has a different aspect ratio than the TRIMET 180 kA cell, and likely has a different mode coupling for the MPI.

Moving forward, we plan on using the mobile model to explore the phase space of the dynamic stabilization of the cell [4, 10]. In particular, we are interested in looking at the stabilization effect of adding an oscillating vertical magnetic flux density at different oscillation frequencies and amplitudes.

5. References

1. Ibrahim Mohammad, Marc Dupuis, and Douglas Kelley, A New Mechanical Model of Magnetohydrodynamic Instabilities in Aluminium Electrolysis Cells, *Proceedings of 41st International ICSOBA Conference*, Dubai, UAE, 5–9 November 2023, Paper AL52, *TRAVAUX* 44, 1763–1772.
2. Jean-Frédéric Gerbeau, Claude Le Bris, and Tony Lelièvre, *Mathematical Methods for the Magnetohydrodynamics of Liquid Metals*, Oxford University Press, 2006.
3. P. A. Davidson and R. I. Lindsay, Stability of interfacial waves in aluminium reduction cells, *J. Fluid Mech.* 362, 1998, 273-295.
4. Ibrahim Mohammad et al., Oscillating currents stabilize aluminum cells for efficient, low carbon production, *JOM* 74, 2022, 1908-1915.
5. Valdis Bojarevics and Marc Dupuis, MHD Stability of Aluminium Cells - Cathode Design Effects, *Light Metals* 2024, 746-753.
6. Valdis Bojarevics and J.W. Evans, Mathematical Modelling of Hall-Heroult Pot Instability and Verification of Measurements of Anode Current Distribution, *Light Metals* 2015, 783-788.
7. Valdis Bojarevics, E. Radionov, and Y. Tretiyakov, Anode bottom burnout shape and velocity field investigation in high amperage electrolysis cell, *Light Metals* 2018, 551-556.
8. V. Bojarevics and M. V. Romerio, Long waves instability of liquid metal-electrolyte interface in aluminium electrolysis cells: a generalization of Sele's criterion, *Eur. J. Mech B/Fluids* 13, 1994, 33-56.
9. MathWorks, Fit curve or surface to data, MATLAB documentation,

https://www.mathworks.com/help/curvefit/fit.html (Accessed on 26 July 2024).

10. Marc Dupuis and Valdis Bojarevics, Stabilizing aluminium reduction cells by oscillating currents in magnetic compensation loops, *Proceedings of 40th International ICSOBA Conference*, Athens, Greece, 10 - 14 October 2022, Paper AL 20, *TRAVAUX* 51, 1243-1254.